Partial-epitaxial morphology of graphene nanoribbon on the Si-terminated SiC(0001) surfaces

V. Sorkin* and Y. W. Zhang
Institute of High Performance Computing, Singapore 138632, Singapore
(Received 14 October 2009; revised manuscript received 14 January 2010; published 24 February 2010)

We present a study of morphology of graphene nanoribbons with armchair edges placed on the SiC(0001) substrates. We found that on the Si-terminated SiC(0001) surface the initial planar shape of a graphene nanoribbon can be substantially distorted by the underlying substrate. Appreciable ripples are created in the graphene nanoribbon due to the combined effect of the van der Waals interaction and covalent bond formation between the graphene nanoribbon and the substrate. A graphene nanoribbon with a narrow width forms covalent bonds only along the edges, creating a partial wavy cylindrical shape of the nanoribbon. With an increase in the nanoribbon width, covalent bonds are formed not only along the edges but also in the interior, resulting in a reduction in the distortion and a decrease in the amplitude of the ripples. It is also found that the number of covalent bonds between the graphene nanoribbon and the substrate grows initially and then saturates as the temperature increases. On the C-terminated SiC(0001) substrates, the planar shape of the graphene nanoribbon is retained due to the absence of covalent bond formation at the interface.

DOI: 10.1103/PhysRevB.81.085435 PACS number(s): 64.70.Nd, 61.46.−w, 68.37.Ef

I. INTRODUCTION

Graphene[1,2] is a one-atom-thick allotrope of carbon, which has been actively explored recently.[3] This is a material of considerable interest for many potential applications in the next generation of nanoelectonics.[4–7] Two methods are in use today to produce graphene: mechanical exfoliation (repeated peeling) of graphite layers[8,9] and epitaxial growth.[10,11] Epitaxial growth produces high-quality samples of graphene accommodated on a SiC substrate. Most of the electrical and mechanical properties of graphene relevant for nanoelectonics devices are directly related to its structure and morphology, which can be modified by a substrate. Thus, it is essential to understand the effect of a substrate on the supported graphene.

Modification of the graphene morphology due to its interaction with the underlying substrate was for the first time experimentally observed by Ishigami *et al.*[12] They employed scanning probe microscopy to study a graphene sheet supported by silicon dioxide. Significant spatial perturbations breaking the hexagonal lattice symmetry of graphene were observed. Recently, Geringer *et al.*[13] demonstrated that the intrinsic rippling observed on artificially suspended graphene can exist as well, if graphene is directly deposited on SiO_2. Using scanning tunneling microscopy, Usachov *et al.*[14] examined the graphene morphology on the Ni(110) surface and revealed that the strong chemical interaction of carbon with nickel gives rise to a noticeable curving of the graphene layer on a scale of a few angstroms. Stoberl *et al.*[15] investigated by atomic force microscopy the morphology of graphene on GaAs and InGaAs substrates. They concluded that graphene sheets strongly follow the texture of the sustaining substrates independent on doping, polarity, or roughness. Varchon *et al.*[10] applied scanning tunneling microscopy to study interaction between a graphene sheet and the Si-terminated silicon carbide surface of SiC(0001). Their experimental observations and the extensive *ab initio* calculations showed that the Si-terminated SiC substrate modifies the shape of graphene. They found that ripples could be created in the graphene sheet by the underlying substrate. Atomic structure of an infinite graphene sheet on the C-terminated SiC($000\bar{1}$) surface was studied by Magaud *et al.*[11] It was found that graphene is barely affected by the underlying C-terminated substrate and retains its geometry and properties.

The extensive first-principles calculations of Varchon *et al.*[10] and Magaud *et al.*[11] were carried out for an infinite single graphene sheet and were limited to zero temperature. In practical applications only a finite-size graphene sheet supported by a substrate may be used in nanoelectronics devices operating at finite temperatures. Therefore, we studied both the finite-size effects and the effect of temperature on the graphene morphology to gain an in-depth understanding of the issue. In our implementation we examined the morphology of a graphene nanoribbon (a thin strip of graphene) overlying on a silicon carbide substrate at zero and finite temperatures.

The remainder of the paper is organized as follows: our computational model is presented in Sec. II and the results of our calculations are discussed in Sec. III. The conclusions are given in Sec. IV.

II. COMPUTATIONAL MODEL

In our model a silicon carbide substrate was represented by eight carbon-silicon bilayers (see Fig. 1). We examined both the 6H-SiC and 4H-SiC allotropes of silicon carbide

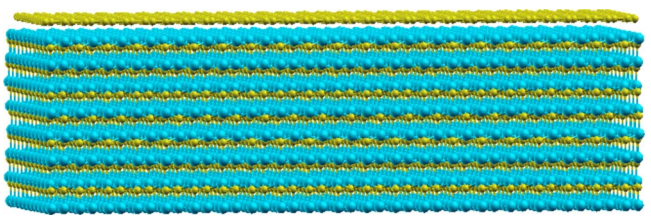

FIG. 1. (Color online) Sample geometry: a graphene nanoribbon on the top of a 6H-SiC(0001) surface.

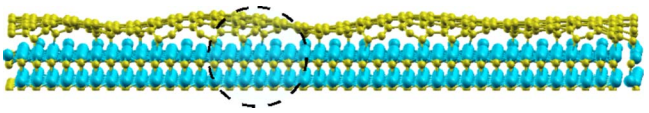

FIG. 2. (Color online) Ripples in a graphene nanoribbon accommodated on the Si-terminated 6H-SiC(0001) surface. The dashed line indicates the region shown on an enlarge scale in Fig. 4.

with the Si-terminated SiC(0001) and the C-terminated SiC($000\bar{1}$) surfaces.

A graphene nanoribbon with armchair edges is infinite along the X direction and finite along the Y direction was placed on a SiC(0001) substrate. Periodic boundary conditions were applied along the X and the Y directions. Two SiC bilayers were fixed at the bottom of the sample to mimic a semi-infinite substrate. The width of the graphene nanoribbon, W, was varied between $W=26.4$ and 53.51 Å. The substrate size was changed to adapt to the width variation accordingly. The number of atoms in the 6H-SiC(0001) sample was varied from $N=2901$ up to $N=5811$ and from $N=2032$ up to $N=4047$ in the sample with the 4H-SiC(0001) lattice structure. The distance between the graphene nanoribbon and the substrate was initially set to $Z=2.3$ Å. This distance was chosen to provide the fastest convergence to the total-energy minimum during the conjugate gradient (CG) minimization. We verified that the results of our calculations were independent of this particular choice.

We applied a semiempirical many-body potential introduced by Tersoff[16] to describe the C-C, C-Si, and Si-Si interatomic interactions. This potential was recently successfully employed to study carbon nanotubes[17,18] and fullerenes,[19] silicon nanotubes,[20] and silicon carbide.[21]

CG method was applied to minimize the total energy of the sample at zero temperature. Subsequently we investigated the morphology of a graphene nanoribbon supported by a substrate. Thereafter classical molecular dynamics (MD) was used to study interaction of a graphene nanoribbon with the underlying SiC substrate at finite temperatures. Both CG and MD methods are implemented as a part of the Large-scale Atomic/Molecular Massively Parallel Simulator code,[22] which was used in our simulations.

III. RESULTS AND DISCUSSION

At first we placed a graphene nanoribbon on the Si-terminated 6H-SiC(0001) surface and minimized the total energy of the system at zero temperature. As can be seen from Fig. 2 the shape of the planar graphene nanoribbon is apparently altered by the substrate and ripples appear when the minimum-energy configuration is reached. Similarly, the initial planar shape of a graphene nanoribbon was also distorted when it was overlying on the Si-terminated 4H-SiC(0001) surface.

The average amplitude of the ripples in the graphene nanoribbon is about 1 Å (see Fig. 3). The wavelength of the ripples, estimated as the distance between two consequent ripple crests, is about ~20 Å as shown in Fig. 3.

We find that the ripples are mainly due to the combined effect of the van der Waals repulsion and covalent bond formation between the graphene nanoribbon and substrate. In Fig. 4 an atomic configuration (indicated by the dashed line in Fig. 2) around a new bond formed by a C atom of the graphene nanoribbon and a Si atom of the substrate is visualized. The Si-C pair, shown in Fig. 4, establishes a covalent bond since the distance between the two atoms is $d_{\text{Si-C}}=1.85$ Å. This length is sufficiently close to the covalent bond length in silicon carbide $d_{\text{Si-C}}=1.89$ Å.[23] Note that the distance from the C atom of the Si-C bond to its nearest graphene neighbors increases from the initial bond length $d_{\text{C-C}}=1.4$ Å to the final one $d_{\text{C-C}}=1.52$ Å. This length is very close to the sp^3 covalent bond length in diamond $d_{\text{C-C}}=1.54$ Å.[23] Moreover, the bond angle formed by the triplets of graphene atoms around the Si-C bond ($\angle\text{ABC}=108.1°$) is close to the sp^3 bond angle 109.5° (Ref. 23) (see Fig. 4). The bond angles of the C-C-Si triplets $\angle\text{ABD}=\angle\text{CBD}=108.4°$ are also close to the sp^3 bond angle. Hence, the above results clearly demonstrate that covalent bonds have formed between the graphene nanoribbon and the substrate.

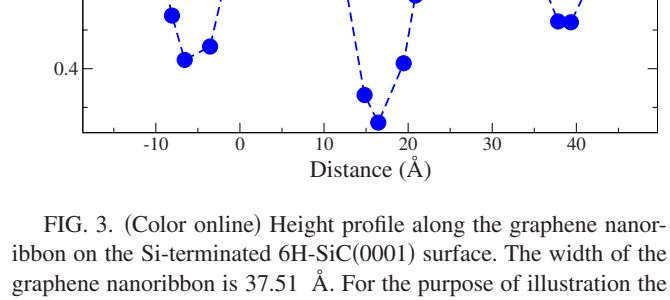

FIG. 3. (Color online) Height profile along the graphene nanoribbon on the Si-terminated 6H-SiC(0001) surface. The width of the graphene nanoribbon is 37.51 Å. For the purpose of illustration the zero height is set at the absolute minimum of the height profile.

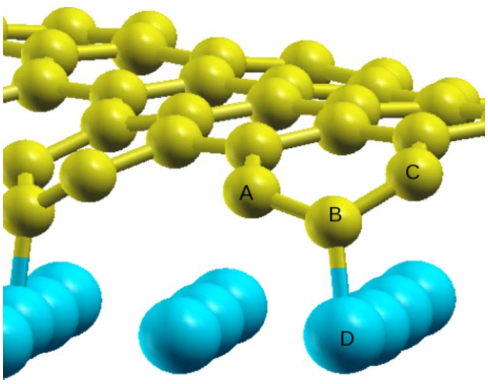

FIG. 4. (Color online) An atomic configuration around a covalent bond formed between the graphene nanoribbon and the underlying 6H-SiC(0001) substrate. The C-Si bond length $|\text{BD}|=1.85$ Å, and the C-C bond lengths $|\text{AB}|$ and $|\text{BC}|=1.52$ Å. The bond angles $\angle\text{ABD}$ and $\angle\text{CBD}=108.4°$, and $\angle\text{ABC}=108.1°$.

As we mentioned above the amplitude of the ripples in a graphene nanoribbon on the underlying substrate is about $\simeq 1$ Å. We estimated this amplitude as one half of the difference between the highest and the lowest points in the height profile (see Fig. 3). As a covalent Si-C bond is formed, the distance from the C atom of the bond to the SiC substrate is roughly equal to the length of the bond 1.85 Å. This is the lowest point of the height profile. It should be noted that the equilibrium distance (~ 3.1 Å) of the van der Waals between the graphene nanoribbon and substrate is much larger than the Si-C bond length. As a result, repulsion occurs near the bonding site between the graphene nanoring and the substrate. Hence, the out-of-plane bending takes place near the bonding site. Since the characteristic length (cutoff radius) of the van der Waals interaction in the present model is about $\simeq 3.7$ Å, this determines the highest point in the height profile. Using these two heights we estimated the amplitude of the ripples in the nanoribbon to be about $\simeq 1$ Å.

We have shown that covalent bonds are formed between the surface Si atoms and the graphene nanoribbon C atoms. During the Si-C bond formation, its average Si-C bond ($E_{\text{C-Si}}=6.34$ eV per atom[24]) is larger than the average Si-Si bond ($E_{\text{Si-Si}}=4.63$ eV per atom).[25] However the formation of Si-C bonds comes at the expense of the sp^2 to sp^3 hybridization of the C-C bonds of the graphene nanoribbon and the nanoribbon bending, which is energetically unfavored. In addition, it is also necessary to overcome the van der Waals repulsion. Hence, the formation of a new Si-C bond is possible until the energy gain from the Si-C bond formation is not offset by the cost of an additional sp^2 to sp^3 hybridization, by increase in the strain energy of the nanoribbon and by the van der Waals repulsion. As a trade-off, only a limited number of carbon atoms of the graphene nanoribbon form C-Si bonds. Since only a restricted number of the carbon atoms links the graphene nanoribbon to the underlying SiC substrate, the epitaxy is partial.

It should be mentioned that the ripple wavelength of the nanoribbon is related to the periodicity in the bond formation between the nanoribbon and the substrate. Based on the analysis of the minimum-energy configuration we found that Si-C bonds are established between the pairs of carbon and silicon atoms which are initially aligned one above the other. In the initial configuration the difference in the X coordinates of the pairs forming Si-C bonds between the graphene nanoribbon and the 6H-SiC(0001) substrate is less than $\Delta x=0.15$ Å. The difference in the Y coordinates is less than $\Delta y=0.13$ Å. [$\Delta x=0.11$ Å and $\Delta y=0.19$ Å for the 4H-SiC(0001) substrate]. Given the positions of the initially aligned atom pairs we found the ripple wavelength to be $\lambda=21.3$ Å.

The ripple formation mechanism considered above is not unique to the 6H-SiC(0001) substrate. Ripples are also introduced in the same way in a graphene nanoribbon located on the Si-terminated 4H-SiC(0001) substrate.

As can be seen in Fig. 5(a), a graphene nanoribbon with the width $W=26.4$ Å only forms covalent bonds along the graphene nanoribbon edges. Due to the combined effect of the van der Waals repulsion and the covalent bond formation the graphene nanoribbon acquires a partial cylindrical shape,

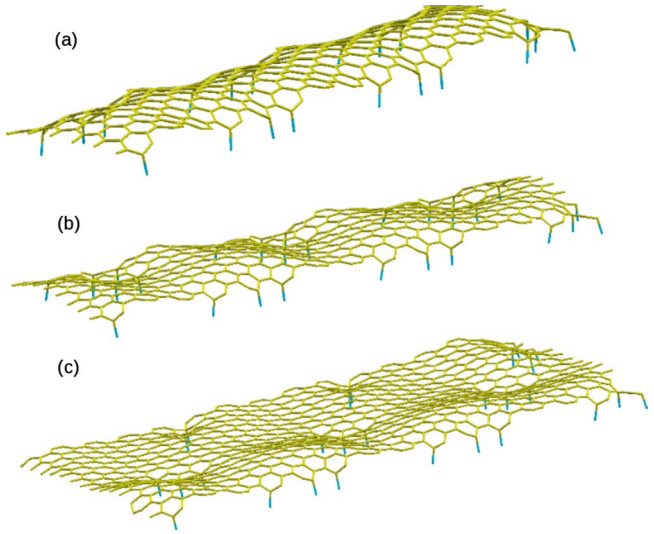

FIG. 5. (Color online) Morphology of a graphene nanoribbon on a 6H-SiC(0001) surface as a function of the lateral width: (a) $W=26.4$ Å, (b) $W=31.75$ Å, and (c) $W=47.76$ Å.

resembling a segment of a carbon nanotube distorted by ripples. This immediately raises the question of whether this shape is specific to the chosen width of the graphene nanoribbon. To answer this question, we increased the width up to $W=47.76$ Å and examined the morphology of the graphene nanoribbon. We found that when the width was increased, covalent bonds are formed not only along the edge of the nanoribbon but also in the interior. Such bond arrangement change induces a noticeably different ripple configuration, which does not resemble a segment of a partial nanotube [see Figs. 5(b) and 5(c)]. Furthermore, we did not detect any marked changes in the overall shape of the graphene nanoribbon as we increased its width, albeit the moderate reduction in the amplitude of the ripples (see Fig. 7). The overall shape of the graphene nanoribbon on the Si-terminated 4H-SiC(0001) surface (see Fig. 6) also varies insignificantly with the width. The most noticeable effect is a decrease in the amplitude of the ripples with an increase in the nanoribbon width due to the additional interior covalent bond formation (see Fig. 7).

We also note that the ripple wavelength was estimated only for narrow graphene nanoribbons which attain sinelike-

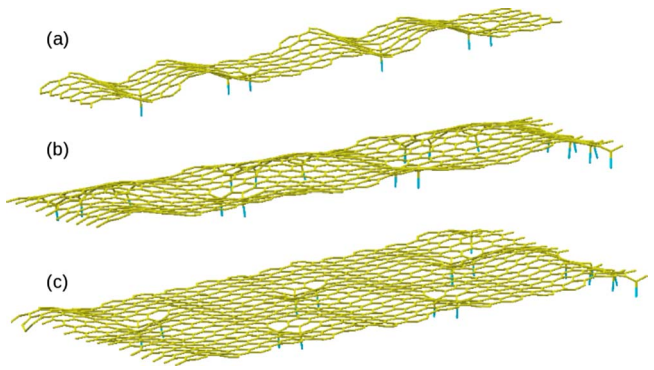

FIG. 6. (Color online) Morphology of a graphene nanoribbon on a 4H-SiC(0001) surface as a function of the lateral width: (a) $W=29.36$ Å, (b) $W=37.51$ Å, and (c) $W=53.51$ Å.

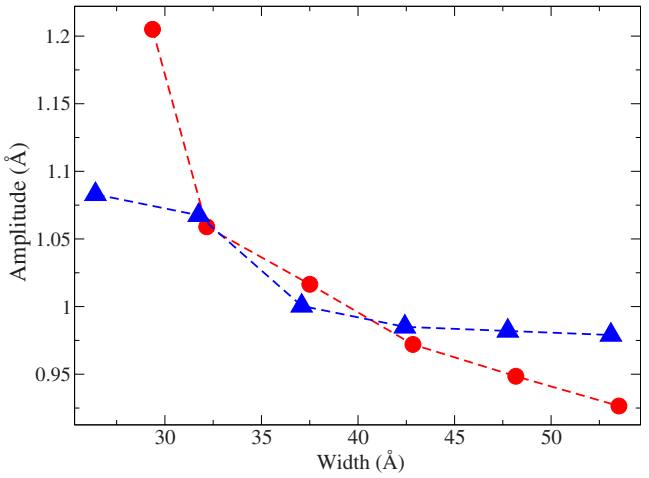

FIG. 7. (Color online) Amplitude of the ripples in a graphene nanoribbon on the Si-terminated 6H-SiC(0001) (triangles) and 4H-SiC(0001) (circles) surface as a function of the nanoribbon width.

wave shape on the underlying SiC substrate. When the width of graphene nanoribbon was increased further, additional covalent bonds were formed in the nanoribbon interior, thus changing its wave patterns. The wide nanoribbons attain a complex pattern with interior and edge regions distinct from each other. As a result the shape of wide nanoribbons cannot be approximated by a simple sinelike wave with a uniquely determined wavelength.

It should be pointed out that the ripple formation mechanism considered here is totally different from the one for a free-standing graphene nanoribbon, where ripples are induced by edge tension.[26] In a free-standing graphene nanoribbon, compressive edge stresses along the edges of the graphene nanoribbon may cause out-of-plane warping or ripples even at zero temperature.[26] In contrast, the ripples in a graphene nanoribbon on the SiC substrate are due to covalent bond formation and van der Waals repulsion between the graphene nanoribbon and the substrate.

The effect of temperature on the morphology of a graphene nanoribbon placed on a SiC(0001) substrate was also studied. The graphene nanoribbon and the underlying substrate were equilibrated at temperatures from $T=500$ K up to $T=3500$ K. It was found that the number of the Si-C bonds formed between the graphene nanoribbon and the Si-terminated surface initially increases with the temperature [see Figs. 8(a) and 8(b) and Figs. 9(a) and 9(b)]. The number of newly formed bonds grows initially since the energetic barriers, which hinder the bond formation, are effectively reduced at the elevated temperature. Above the $T=1500$ K the average number of the established bonds remains constant (see Fig. 10). At even higher temperatures, as shown in Figs. 8(c) and 9(c), various structural defects start to emerge in the graphene nanoribbon. In addition, the effect of temperature on the ripple amplitude was studied. For narrow nanoribbons a moderate increase in the ripple amplitude was observed as temperature was raised due to the combined effect of additional bond formation at the interface and thermal fluctuations. However, above $T=1500$ K the ripple amplitude stabilizes, as does the number of covalent bonds at the

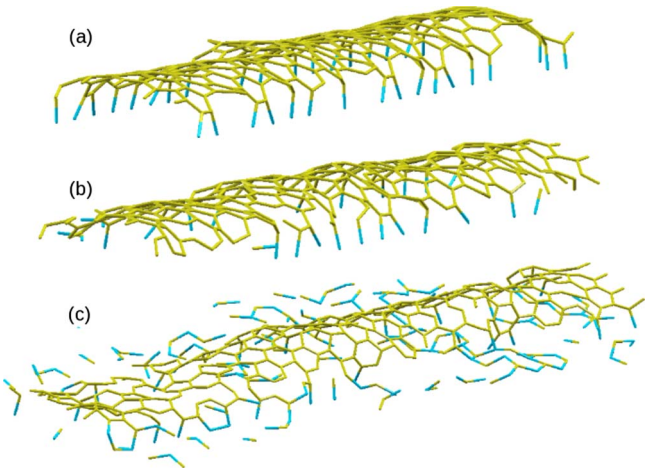

FIG. 8. (Color online) Morphology of the graphene nanoribbon on the 6H-SiC(0001) surface as a function of temperature: (a) $T=500$ K, (b) $T=1500$ K, and (c) $T=3500$ K. Width of the graphene nanoribbon is 26.4 Å.

nanoribbon-substrate interface (see Fig. 11). The additional covalent bonds formed along the armchair edges force the interior nanoribbon atoms to move further in the out-of-plane direction. This further increases the ripple amplitude of narrow nanoribbons. In the case of wide nanoribbons, additional covalent bonds formed in the nanoribbon interior merely reduce the ripple amplitude. The relationship between ripple wavelength and temperature was also investigated. We found that with an increase in temperature, the sine-wavelike shape of narrow graphene nanoribbons is significantly distorted by thermal fluctuations, causing structural defects and additional covalent bonds formed at the nanoribbon-substrate interface. Thus it is difficult to define the ripple wavelength, let alone to calculate it as a function of temperature.

In addition, we investigated the morphology of a graphene nanoribbon on the C-terminated 4H-SiC$(000\bar{1})$ and 6H-SiC$(000\bar{1})$ surfaces. We found that the van der Waals repulsion and the energy cost of hybridization of the graphene C-C bonds from sp^2 to sp^3 to form C-C bonds with

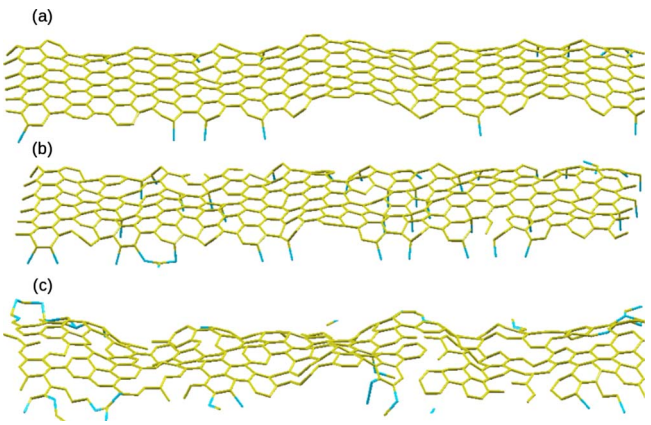

FIG. 9. (Color online) Morphology of the graphene nanoribbon on the 4H-SiC(0001) surface as a function of temperature: (a) $T=500$ K, (b) $T=1500$ K, and (c) $T=3500$ K. Width of the graphene nanoribbon is 29.36 Å.

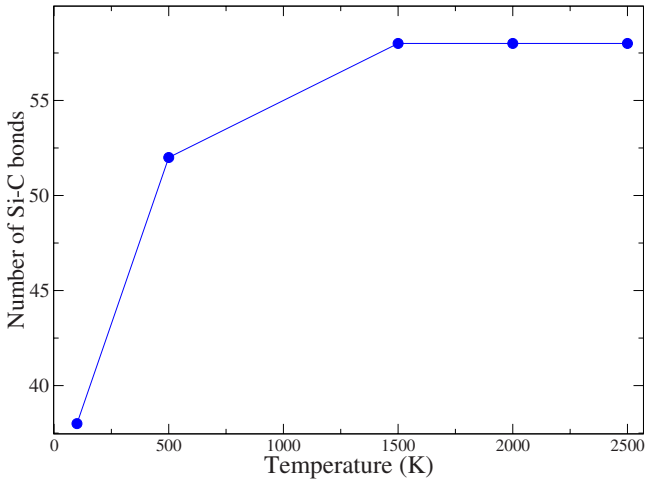

FIG. 10. (Color online) Number of Si-C bonds at the nanoribbon-6H-SiC(0001) substrate interface as a function of temperature. Width of the graphene nanoribbon is 26.4 Å.

the underlying substrate exceeds the energy gain due to saturation of the surface dangling bonds. Therefore, the ripples are absent in the graphene nanoribbon. We did not observe the edge stress-induced ripples[26] as well, considering that the size of our computational box was less than the wavelength of these intrinsic ripples. Hence, contrary to the case of the SiC(0001) surface, the planar shape of the graphene nanoribbon on the SiC($000\bar{1}$) surface is retained. We have also performed a preliminary study on the effect of the edge type. It was found that ripples also emerge in nanoribbons with zigzag edge. This should not take as a surprise since chemical bonds are also formed between the graphene and the substrate. However, the number of bonds per unit edge length for the nanoribbon with armchair edges is higher than that of the nanoribbon with zigzag edges. This is especially noticeable when narrow nanoribbons are considered, as

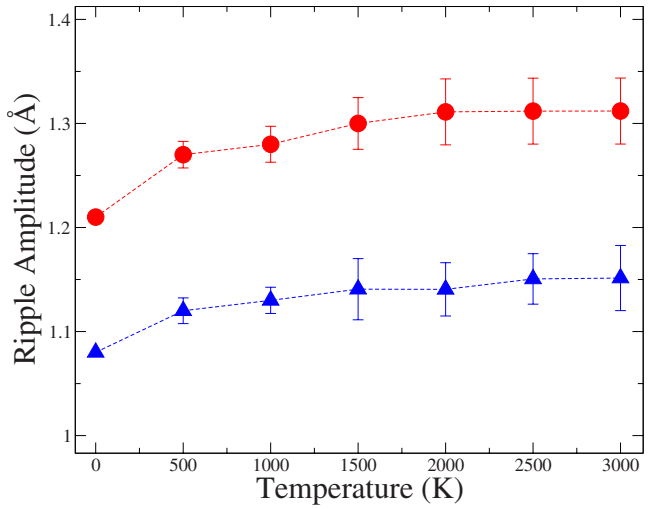

FIG. 11. (Color online) Ripple amplitude of the graphene nanoribbon with the width of 29.36 Å on the Si-terminated 4H-SiC(0001) substrate (circles) and the graphene nanoribbon with the width of 26.4 Å on the Si-terminated 6H-SiC(0001) substrate (triangles) as a function of temperature.

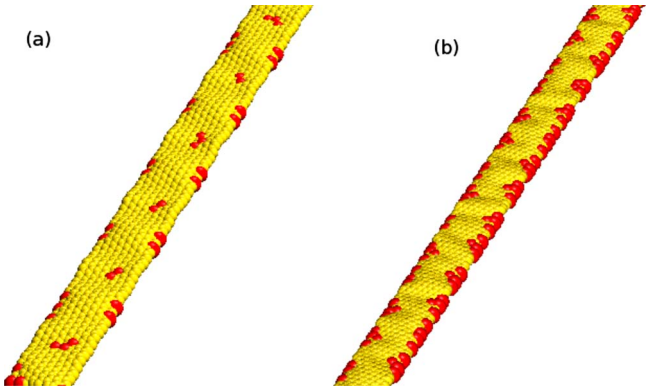

FIG. 12. (Color online) Ripples in a graphene nanoribbon accommodated on the Si-terminated 6H-SiC(0001) surface. Carbon atoms forming covalent bonds with the underlying substrate are marked. (a) Graphene nanoribbon with zigzag edges, width 15.6 Å. (b) Graphene nanoribbon with armchair edges, width 15.9 Å.

shown in Fig. 12 where the graphene atoms forming covalent bonds with the underlying SiC(0001) substrate are marked. Therefore ripple amplitude and wavelength are different for nanoribbons with these two different types of edge.

The recently available experimental data are obtained at high temperatures ($T > 1300$ K) for graphene sheets on a reconstructed SiC(0001) surface.[27] These experimental data indicate a strong covalent interaction between the Si-terminated SiC substrate and graphene. Typical distance measured between graphene and substrate is about 2 Å. As a result of covalent bonding at the graphene-substrate interface ripples with the amplitude about 0.6–1.2 Å and the wavelength of about 20 Å emerge in graphene.[27] Although these measurements cannot be directly compared with the case of a graphene nanoribbon accommodated on the Si-terminated unreconstructed SiC(0001) surface at low temperatures, the calculated ripple amplitude and its wavelength are close to the experimentally measured. Thus the experimental and the present simulation results share two important features: the chemical bond formation and ripple formation.

IV. CONCLUSIONS

In this paper we studied morphology of a graphene nanoribbon accommodated on a 6H-SiC(0001) [and a 4H-SiC(0001)] surface using a semiempirical many-body potential introduced by Tersoff. We found that the planar shape of the graphene nanoribbon is altered in the presence of the SiC substrate. Small ripples are introduced in the graphene nanoribbon as a result of covalent bonding between the C atoms of the nanoribbon and the Si atoms of the substrate and van der Waals repulsion between the nanoribbon and the substrate.

On the 6H-SiC(0001) surface, the shape of the graphene nanoribbon depends to some extent on its width. When the width is narrow the graphene nanoribbon form covalent bonds only along the nanoribbon edges. The nanoribbon acquires a wavy cylindrical shape, resembling a segment of a single wall carbon nanotube. As the width increases the planar shape of the graphene nanoribbon becomes less distorted

by the ripples due to the covalent bond formation in the interior of the nanoribbon. A partial epitaxy exists since only a limited number of the graphene nanoribbon atoms participate in Si-C bond formation with the silicon atoms of the underlying substrate.

In addition, the effect of temperature on the morphology of a graphene nanoribbon placed on a SiC substrate was also examined. We found that number of covalent bonds formed between the graphene nanoribbon and the surface increases initially and then saturates at higher temperatures. The above understandings can also be applied to the 4H-SiC(0001) surface.

Finally, as opposed to the Si-terminated SiC(0001) case, covalent bonds are not formed between the C-terminated SiC($000\bar{1}$) substrate and a graphene nanoribbon. Hence, the C-terminated SiC($000\bar{1}$) surface has little influence on the planar shape of a graphene nanoribbon.

ACKNOWLEDGMENTS

The authors thank Haibin SU and A. Sorkin for fruitful and stimulating discussions. This work was funded by the Agency for Science, Research and Technology (A*STAR), Singapore. Graphic images were made with the XCRYSDEN visualization package, developed by A. Kokalj (Ref. 28). The Large-scale Atomic/Molecular Massively Parallel Simulator (LAMMPS) (Ref. 22) code used in our simulations was distributed by Sandia National Laboratories.

*sorkinv@ihpc.a-star.edu.sg

[1] K. S. Novoselov, A. K. Geim, S. V. Morozov, D. Jiang, Y. Zhang, S. V. Dubonos, I. V. Grigorieva, and A. A. Firsov, Science **306**, 666 (2004).
[2] J. C. Meyer, A. K. Geim, M. I. Katsnelson, K. S. Novoselov, T. J. Booth, and S. Roth, Nature (London) **446**, 63 (2007).
[3] A. H. Castro Neto, F. Guinea, N. M. R. Peres, K. S. Novoselov, and A. K. Geim, Rev. Mod. Phys. **81**, 109 (2009).
[4] C. Berger, Z. Song, T. Li, X. Li, A. Y. Ogbazghi, R. Feng, Z. Dai, A. N. Marchenkov, E. H. Conrad, P. N. First, and Walt A. de Heer, J. Phys. Chem. B **108**, 19912 (2004).
[5] A. K. Geim and K. S. Novoselov, Nature Mater. **6**, 183 (2007).
[6] J. Moon, D. Curtis, D. W. M. Hu, C. McGuire, P. Campbell, G. Jernigan, J. Tedesco, B. VanMil, R. Myers-Ward, and C. Eddy, IEEE Electron Device Lett. **30**, 650 (2009).
[7] P. Sutter, Nature Mater. **8**, 171 (2009).
[8] K. S. Novoselov, A. K. Geim, S. V. Morozov, D. Jiang, M. I. Katsnelson, I. V. Grigorieva, S. V. Dubonos, and A. A. Firsov, Nature (London) **438**, 197 (2005).
[9] Y. Zhang, Y.-W. Tan, H. L. Stormer, and P. Kim, Nature (London) **438**, 201 (2005).
[10] F. Varchon, P. Mallet, J.-Y. Veuillen, and L. Magaud, Phys. Rev. B **77**, 235412 (2008).
[11] L. Magaud, F. Hiebel, F. Varchon, P. Mallet, and J.-Y. Veuillen, Phys. Rev. B **79**, 161405(R) (2009).
[12] M. Ishigami, J. H. Chen, W. G. Cullen, M. S. Fuhrer, and E. D. Williams, Nano Lett. **7**, 1643 (2007).
[13] V. Geringer, M. Liebmann, T. Echtermeyer, S. Runte, M. Schmidt, R. Ruckamp, M. C. Lemme, and M. Morgenstern, Phys. Rev. Lett. **102**, 076102 (2009).
[14] D. Usachov, A. M. Dobrotvorskii, A. Varykhalov, O. Rader, W. Gudat, A. M. Shikin, and V. K. Adamchuk, Phys. Rev. B **78**, 085403 (2008).
[15] U. Stoberl, U. Wurstbauer, W. Wegscheider, D. Weiss, and J. Eroms, Appl. Phys. Lett. **93**, 051906 (2008).
[16] J. Tersoff, Phys. Rev. B **39**, 5566 (1989).
[17] J. Zang, A. Treibergs, Y. Han, and F. Liu, Phys. Rev. Lett. **92**, 105501 (2004).
[18] M. J. Lopez, I. Cabria, N. H. March, and J. A. Alonso, Carbon **43**, 1371 (2005).
[19] E. B. Halac, M. Reinoso, A. G. Dall'Asen, and E. Burgos, Phys. Rev. B **71**, 115431 (2005).
[20] J. W. Kang, J. J. Seo, and H. J. Hwang, J. Nanosci. Nanotechnol. **2**, 687 (2002).
[21] V. I. Ivashchenko, P. E. A. Turchi, V. I. Shevchenko, and O. A. Shramko, Phys. Rev. B **70**, 115201 (2004).
[22] S. J. Plimpton, J. Comput. Phys. **117**, 1 (1995).
[23] P. Mélinon, B. Masenelli, F. Tournus, and A. Perez, Nature Mater. **6**, 479 (2007).
[24] P. Kackell, B. Wenzien, and F. Bechstedt, Phys. Rev. B **50**, 17037 (1994).
[25] D. Alfe, M. J. Gillan, M. D. Towler, and R. J. Needs, Phys. Rev. B **70**, 214102 (2004).
[26] V. B. Shenoy, C. D. Reddy, A. Ramasubramaniam, and Y. W. Zhang, Phys. Rev. Lett. **101**, 245501 (2008).
[27] J. Borysiuk, R. Bozek, W. Strupinski, A. Wysmolek, K. Grodecki, R. Stepniewski, and J. M. Baranowski, J. Appl. Phys. **105**, 023503 (2009).
[28] A. Kokalj, Comput. Mater. Sci. **28**, 155 (2003).